THE UNIVERSITY *of* EDINBURGH

Edinburgh Research Explorer

Transverse anisotropy in the mixed-valent (Mn2Mn4Mn3IV)-Mn-II-Mn-III single-molecule magnet

OPEN ACCESS

Transverse anisotropy in the mixed-valent Mn2IIMn4IIIMn3IV single-molecule magnet

Saiti Datta, Constantinos J. Milios, Euan Brechin, and Stephen Hill

Additional information on J. Appl. Phys.

Transverse anisotropy in the mixed-valent $Mn_2^{II}Mn_4^{III}Mn_3^{IV}$ single-molecule magnet

Saiti Datta,[1,a)] Constantinos J. Milios,[2] Euan Brechin,[2] and Stephen Hill[1]

[1]*Department of Physics, University of Florida, Gainesville, Florida 32611, USA*
[2]*School of Chemistry, University of Edinburgh, West Mains Road, Edinburgh, EH9 3JJ, United Kingdom*

High-frequency electron paramagnetic resonance measurements have been performed on a single-crystal sample of a recently discovered mixed valent $Mn_2^{II}Mn_4^{III}Mn_3^{IV}$ single-molecule magnet, with a spin $S = 17/2$ ground state. Frequency, temperature and field-orientation dependent studies confirm previously reported axial magnetic anisotropy parameters and also provide clear evidence for higher order (fourth and sixth) transverse terms that are responsible for the magnetic quantum tunneling observed in this system. © *2008 American Institute of Physics.*
[DOI: 10.1063/1.2838339]

INTRODUCTION

Mixed-valent manganese clusters are considered ideal candidates for single-molecule magnets (SMMs) as they often (a) exhibit large spin ground states and (b) possess Jahn–Teller distorted Mn_3^{III} ions which contribute to a large easy-axis-type magnetic anisotropy.[1] These nanosized magnetic materials display magnetization hysteresis and quantum tunneling of magnetization[2,3] (QTM) suggesting that they may one day find applications in information storage and possibly quantum computation.

Here, we present single-crystal high-frequency electron paramagnetic resonance (HFEPR) studies of a mixed valent $Mn_2^{II}Mn_4^{III}Mn_3^{IV}$ complex [hereafter Mn_9 (Ref. 4)], confirming the main findings of previous magnetic measurements and inelastic neutron scattering (INS) studies, which showed that Mn_9 has a spin ground state of $S = 17/2$, a dominant axial anisotropy parameterized by a D of value -0.24 cm^{-1}, together with a fourth-order axial zero-field splitting (ZFS) term $B_4^0 = +6.68 \times 10^{-6}$ cm^{-1}. Crucially, the present study provides clear evidence for higher-order (fourth and even sixth order) transverse anisotropy terms, which will clearly influence the tunneling.

EXPERIMENTAL

The $[Mn_9O_7(O_2CCH_3)_{11}(thme)(py)_3(H_2O)_2]$ complex was prepared as reported previously.[4,5] Good sized black crystals were obtained for single-crystal HFEPR measurements. The metallic skeleton of the complex can be thought to comprise two rings: a smaller $[Mn_3^{IV}O]^{10+}$ triangle within a $[Mn_4^{III}Mn_2^{II}O_6]^{4+}$ hexagon (the charge is compensated by the ligands). At first sight, the magnetic core appears to have a pseudothreefold topology. However, closer inspection of the Mn valence states on the outer hexagon reveal a much lower symmetry.[5] All of the Mn ions are in distorted octahedral geometries with the Jahn–Teller elongation of the Mn^{3+} ions lying almost perpendicular to the plane of the

a)Electronic mail: saiti@ufl.edu.

$[Mn_4^{III}Mn_2^{II}O_6]^{4+}$ hexagon. The complex crystallizes such that there are two symmetry-equivalent, but differently oriented molecules in the unit cell whose magnetic easy axes are approximately perpendicular to each other.

HFEPR experiments were performed on a single crystal at various temperatures and frequencies from 50 to 200 GHz with the dc magnetic field applied along different crystallographic directions. The spectra were obtained at fixed frequencies and temperatures while varying the strength of the dc magnetic field. Details of the experimental technique can be found elsewhere.[6,7]

DATA AND DISCUSSION

Single-axis rotation studies were first performed to roughly determine the orientation of the crystal in the magnetic field. Figure 1 shows temperature dependent spectra obtained at 120 GHz, with the field oriented reasonably close (30°) to the easy axis associated with one of the two sites in the unit cell. The intensities of the lowest field peaks decrease upon increasing the temperature. This can be ex-
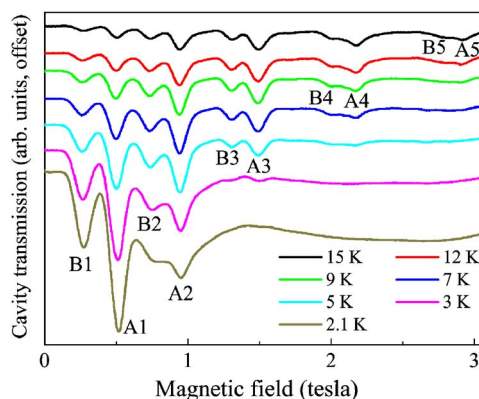

FIG. 1. (Color online) Temperature dependent EPR spectra obtained at 120 GHz with the field oriented reasonably close (30°) to the easy axis of one of the two molecular orientations. Each set of fine structures is further split into peaks labeled A and B, corresponding to inequivalent molecular species with slightly different ZFS parameters (D). See main text for explanation of numbering.
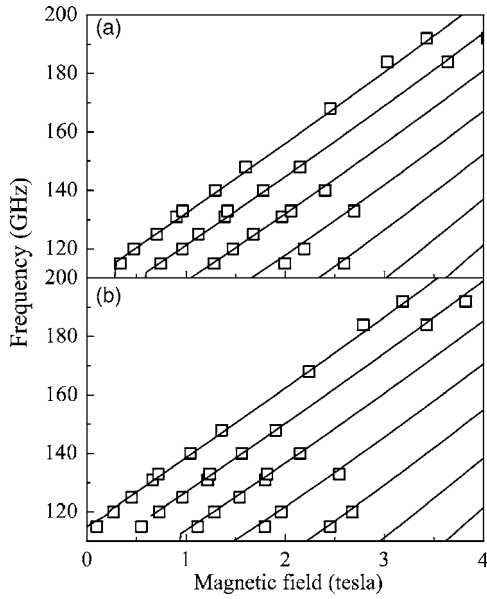
FIG. 2. Frequency dependence of the peak positions (□) associated with the two species: (a) A and (b) B. Data were obtained at 5 K for the same field orientation as in Fig. 1. The solid lines are simulations based on Eq. (1), using the parameters given in the main text.
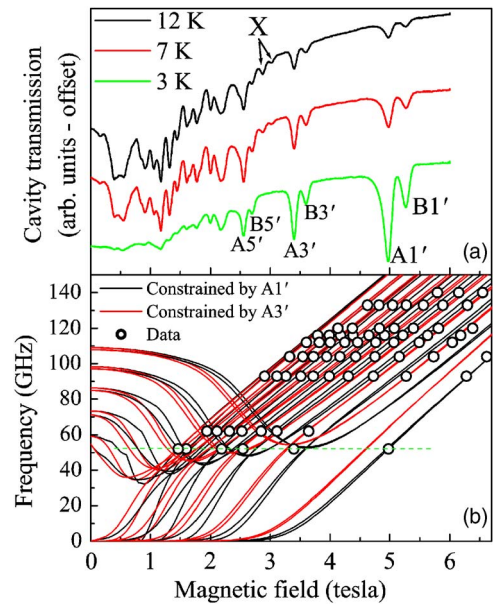

FIG. 3. (Color online) (a) Temperature dependent EPR spectra obtained at 52 GHz with the field in the hard plane of one of the molecular orientations. The fine structure splitting (A and B peaks) can again be clearly seen (refer to main text for explanation of numbering). At the highest temperature, additional peaks appear (labeled X) which we attribute to excited spin multiplets. (b) Frequency dependence of the 7 K hard plane peak positions (○) associated with species A [the dashed curve corresponds to the data in (a)]. The orientation of the field within the hard plane is not known. The curves correspond to various simulations based on Eq. (1) with the inclusion of a rhombic term $[E(\hat{S}_x^2 - \hat{S}_y^2)]$. See main text for explanation.

plained assuming a negative uniaxial anisotropy ($D < 0$). The appearance of two sets of peaks in Fig. 1 indicates that, in addition to the two different molecular orientations, there exist inequivalent Mn_9 species with slightly different ZFS parameters. We label the stronger peaks A and the weaker ones B. Peaks 1, 2, 3, 4, and 5 correspond to the following fine-structure transitions: $m_S = -\frac{17}{2} \rightarrow -\frac{15}{2}$, $-\frac{15}{2} \rightarrow -\frac{13}{2}$, $-\frac{13}{2} \rightarrow -\frac{11}{2}$, $-\frac{11}{2} \rightarrow -\frac{9}{2}$, and $-\frac{9}{2} \rightarrow -\frac{7}{2}$, respectively, where m_S represents the spin projection along the easy (z) axis of the crystal.

Figures 2(a) and 2(b) display the positions of the observed EPR peaks plotted versus frequency for species A and B, and for the same field orientation as the data displayed in Fig. 1. The solid curves were simulated using the following spin Hamiltonian [Eq. (1)], containing only axial ZFS parameters

$$\hat{H} = D\hat{S}_z^2 + B_4^0[35\hat{S}_z^4 - \{30S(S+1)\}\hat{S}_z^2] + \mu_B \mathbf{B} \cdot \vec{g} \cdot \hat{S}. \quad (1)$$

The simulations assume $S = \frac{17}{2}$, and best overall agreement with the data is obtained with $D = -0.24$ cm^{-1} ($D = -0.25$ cm^{-1}) for species A (species B), $B_4^0 = +6.68 \times 10^{-6}$ cm^{-1} and $g_z = 1.98$. It is well documented that low-field data (especially extrapolations to $B = 0$) obtained for fields close to the easy axis are insensitive to transverse anisotropy terms.[8] As can be seen from Table I, the obtained

axial parameters agree very well with previous magnetic and spectroscopic measurements.[4,5]

Rotation about a single axis guarantees field-alignment in the hard plane, although the orientation of the field within the hard plane is not known. Detailed studies (not shown) allow identification of one or other of the hard plane orientations from the angle dependence of the peak positions (see Ref. 9). Figure 3(a) displays temperature dependent 52 GHz spectra for one of these hard-plane orientations. The A and B peaks are again observed, corresponding to the two species. The reversed ordering of A and B (see Fig. 1) is consistent with Eq. (1). Peaks labeled A1′, A3′, and A5′ (likewise for the B peaks) correspond to the following fine-structure transitions: $m_S = -\frac{17}{2} \rightarrow -\frac{15}{2}$, $-\frac{13}{2} \rightarrow -\frac{11}{2}$, and $-\frac{9}{2} \rightarrow \frac{7}{2}$, respectively, where m_S now represents the spin projection along the (high) magnetic field quantization axis. The low field portion of the figure (fields below A5′) is complicated by absorptions due to the other molecular orientation.

We now argue that fourth and higher-order transverse ZFS interactions are necessary in order to account for these spectra. It is well documented that HFEPR measurements

TABLE I. Comparison between ZFS parameters obtained from these studies (EPR) and the various magnetic measurements reported in (Refs. 4 and 5).

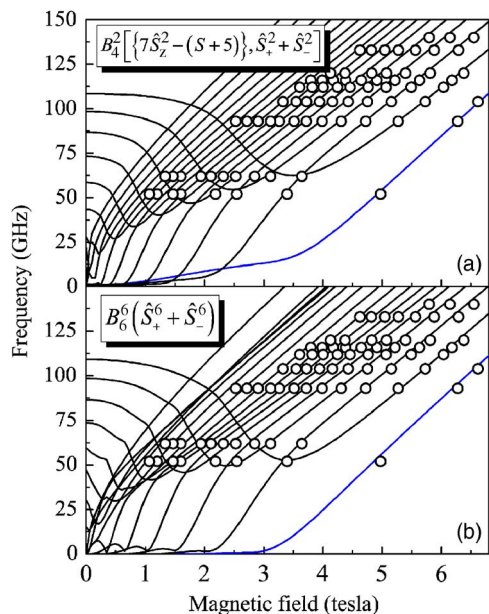| ZFS (cm^{-1})	FDMRS	INS	Magnetization	μ-SQUID	DFT	EPR (A)	EPR (B)
D	−0.247(5)	−0.249(5)	−0.29(3)	−0.258	−0.235	−0.24	−0.25
$B_4^0/10^{-6}$	4.6(1)	7(4)				6.7	6.7

FIG. 4. (Color online) Hard-plane data (from Fig. 3) and simulations based on Eq. (1), with the additional inclusion of the higher-order transverse interactions (a) $B_4^2 \hat{O}_4^2$ and (b) $B_6^6 \hat{O}_6^6$ (actual functions given in the figures). Both simulations agree reasonably well with the experimental data using the axial ZFS parameters determined from the simulations in Fig. 2, along with the following parameters: (a) $B_4^2 = 8.4 \times 10^{-5}$ cm^{-1}, (b) $B_6^6 = 8.4 \times 10^{-7}$ cm^{-1}, and $\phi = 0$ for both (a) and (b). See main text for detailed explanation. The blue curves correspond to the splitting in the ground state $m_S = \pm \frac{17}{2}$ doublet.

with $B \perp c$ provide information concerning transverse terms.[8] In the following analysis, we constrain the axial terms (D and B_4^0) on the basis of the simulations in Fig. 2. Density functional theory (DFT) calculations predict that Mn$_9$ possesses a rhombohedral ZFS parameter $E = 0.035$ cm^{-1}.[5] We find that it is impossible to obtain agreement between our results and simulations including only this interaction $[E(\hat{S}_x^2 - \hat{S}_y^2)]$, as demonstrated in Fig. 3(b). The black curves were generated for two different E values and field orientations relative to the hard axis (within the hard plane): $E = 0.035$ cm^{-1}, $\phi = 25°$; and $E = 0.015$ cm^{-1}, $\phi = 0°$ (i.e., $B \| x$). These parameters were chosen in order to obtain agreement between the simulations and the A1′ peak. However, as can be seen, agreement with A3′ is not good. Conversely, the red curves were generated with the following parameters: $E = 0.035$ cm^{-1}, $\phi = 40°$ and $E = 0.015$ cm^{-1}, $\phi = 38°$ (i.e., $B \| x$). Here, the goal was to achieve agreement with the A3′ peak. g_x and g_y were set to 2.00 for all of these simulations, as well as those in Fig. 4. The main result is that it is *impossible* to obtain anything approaching agreement with more than one of these peaks using only an E parameter.

It turns out that, with the exception of A1′, all EPR peaks are reasonably close to the positions one would expect for extremely weak transverse second order anisotropy (or $\phi = 45°$). In contrast, A1′ is shifted considerably to higher fields. It is only possible to mimic its behavior using higher order transverse terms, as illustrated in Fig. 4. In fact, one can obtain good agreement with the hard-plane spectra for several different parameter sets. Examples are displayed in Fig. 4 involving purely $B_4^2 \hat{O}_4^2$ (a) and $B_6^6 \hat{O}_6^6$ (b). The coefficients are given in the captions. Interestingly, $B_6^6 \hat{O}_6^6$ gives

excellent agreement, whereas terms that one might expect to work well, such as $B_4^3 \hat{O}_4^3$, do not give good agreement. In reality, it is likely that the transverse Hamiltonian involves admixtures of all of these interactions, reflecting the pseudothreefold,[5] albeit low symmetry of the molecule. Only detailed multihigh-frequency measurements performed as a function of the field orientation within the hard plane can resolve this issue, which would be greatly complicated by the multiple species, orientations, and the overall low symmetry of this complex. Nevertheless, the present measurements serve a useful purpose, hinting at the significant fourth (and higher-order) anisotropy that likely results as a consequence of S mixing brought about by low-lying excited spin states.[10] Indeed, the spectra in Fig. 3(a) clearly show features (labeled X) associated with the population of low-lying $S < \frac{17}{2}$ spin states.

One final point to note from Fig. 4(a) is the huge tunnel splitting of the lowest-lying $m_S = \pm \frac{17}{2}$ doublet, which is clearly visible to the naked eye down to low fields. This suggests that a $B_4^2 \hat{O}_4^2$ interaction would cause very fast tunneling in this Mn$_9$ complex, which is not found experimentally and, therefore, seems to be unphysical. Again, this hints at the importance of multiple high-order transverse ZFS interactions that can account for both the EPR data presented here and the slow magnetization dynamics in the quantum regime. We also note that internal dipolar and hyperfine fields must be important for zero-field QTM in these half integer SMMs.

CONCLUSIONS

Multi-high frequency and field orientation dependent EPR studies have enabled a detailed characterization of the spin Hamiltonian of a mixed valent Mn$_9$ complex. These measurements hint at the importance of high- (fourth and sixth) order transverse anisotropy terms in the low temperature quantum dynamics.

ACKNOWLEDGMENTS

[1] D. N. Hendrickson, G. Christou, H. Ishimoto, J. Yoo, E. K. Brechin, A. Yamaguchi, E. M. Rumberger, S. M. J. Aubin, Z. Sun, and G. Aromi, Mol. Cryst. Liq. Cryst. Sci. Technol., Sect. A **376**, 301 (2002).

[2] J. R. Friedman, M. P. Sarachik, J. Tejada, and R. Ziolo, Phys. Rev. Lett. **76**, 3830 (1996).

[3] L. Thomas, F. Lionti, R. Ballou, D. Gatteschi, R. Sessoli, and B. Barbara, Nature (London) **383**, 145 (1996).

[4] E. K. Brechin, M. Soler, J. Davidson, D. N. Hendrickson, S. Parsons, and G. Christou, Chem. Commun. (Cambridge) **19**, 2252 (2002).

[5] S. Piligkos, G. Rajaraman, M. Soler, N. Kirchner, J. V. Slageren, R. Bircher, S. Parsons, H. U. Gudel, J. Kortus, W. Wernsdorfer, G. Christou, and E. K. Brechin, J. Am. Chem. Soc. **127**, 5572 (2005).

[6] M. Mola, S. Hill, P. Goy, and M. Gross, Rev. Sci. Instrum. **71**, 186 (2000).

[7] S. Takahashi and S. Hill, Rev. Sci. Instrum. **76**, 023114 (2005).

[8] E. del Barco, A. D. Kent, S. Hill, J. M. North, N. S. Dalal, E. M. Rumberger, D. N. Hendrickson, N. Chakov, and G. Christou, J. Low Temp. Phys. **140**, 119–174 (2005).

[9] S.-C. Lee, T. C. Stamatatos, S. Hill, S. P. Perlepes, and G. Christou, Polyhedron **26**, 2225 (2007).

[10] A. Wilson, J. Lawrence, E.-C. Yang, M. Nakano, D. N. Hendrickson, and S. Hill, Phys. Rev. B **74**, 140403 (2006).